Introduction to the geometry and growth of normal faults

CONRAD CHILDS[1]*, ROBERT E. HOLDSWORTH[2], CHRISTOPHER A.-L. JACKSON[3], TOM MANZOCCHI[1], JOHN J. WALSH[1] & GRAHAM YIELDING[4]

[1]*Fault Analysis Group, School of Earth Sciences, University College Dublin, Belfield, Dublin 4, Ireland*

[2]*Department of Earth Sciences, University of Durham, South Road, Durham DH1 3LE, UK*

[3]*Basins Research Group, Imperial College, Prince Consort Road, London SW7 2BP, UK*

[4]*Badley Geoscience Ltd, Hundleby, Spilsby, Lincolnshire PE23 5NB, UK*

**Correspondence: conrad.childs@ucd.ie*

Normal faults are the dominant structures found in extensional sedimentary basins developed in continental rifts and passive margins. The geometry and growth of faults are intimately linked, and much of our understanding of how faults grow is derived directly from observations of fault geometry. The key geometric relationship that has underpinned the study of fault growth since the 1980s is the relationship between fault maximum displacement (*D*) and fault length (*L*) as defined by Elliott (1976) and Watterson (1986). This relationship is expressed as $D \alpha L^n$. The value of the exponent n in this relationship has been a topic for discussion for the last 30 years and values ranging between 0.5 and 2.0 have been advocated (e.g. Walsh & Watterson 1988; Cowie & Scholz 1992; Schultz *et al.* 2008). The range of values reflects the natural variation between different areas and uncertainties in data quality and sampling (Gillespie *et al.* 1992; Kim & Sanderson 2005). Irrespective of the value of the exponent, the recognition of a positive correlation between displacement and length suggests that faults grow progressively as their displacement increases (Watterson 1986; Walsh & Watterson 1988).

Since the late 1990s, several studies have been performed in areas where the rate of sedimentation exceeds the fault displacement rate, so that across-fault changes in the thickness of growth strata provide a record of the surface trace length and displacement distribution of faults through time (Morley 1999; Walsh *et al.* 2002; Childs *et al.* 2003; Paton 2006). These studies have shown that evidence for the propagation of normal faults in the geological record is often difficult to find and, in many cases, it appears that the lengths of faults are formed instantaneously within the time resolution of the data. If this is true, then the positive correlation between displacement and length does not define a trend along which individual faults grow. Instead, faults would establish their lengths very early in their development, with initially very low ratios of displacement to length that increase rapidly as displacement accumulates. Which of these models of fault growth is correct remains a matter for debate, as reflected in the content of this volume.

This introduction does not provide a comprehensive review of the literature on this topic, but aims to outline the current models for the growth of faults as a backdrop to the collection of papers in this volume. In the following section, we provide an in-depth description of current models of fault growth. We then discuss the methods by which these can be investigated, highlighting how geometric observations provide constraints on fault growth with reference to the papers published in this volume.

Fault growth models

We consider first the growth of individual faults and later discuss models for the growth of fault systems. Faults have many fractal characteristics (Kakimi 1980; Walsh *et al.* 1991; Marrett & Allmendinger 1992; Wojtal 1994), so that the distinction between faults and fault systems can be dependent on the scale of observation. The processes considered in both – namely, fault initiation, propagation, interaction and linkage – are the same. Despite these considerations, we distinguish between faults and fault systems because the concepts of fault growth were first described in terms of the growth of a single fault and also because the key concerns and the terminology adopted in

From: Childs, C., Holdsworth, R. E., Jackson, C. A.-L., Manzocchi, T., Walsh, J. J. & Yielding, G. (eds) 2017. *The Geometry and Growth of Normal Faults*. Geological Society, London, Special Publications, **439**, 1–9.
First published online September 5, 2017, https://doi.org/10.1144/SP439.24

the literature are different when applied to faults and fault systems.

Growth of an individual fault

The first plots of displacement v. the length of faults were interpreted in terms of the growth of a single fault plane (e.g. Watterson 1986; Walsh & Watterson 1988; Dawers *et al.* 1993). Walsh & Watterson (1989) showed that individual faults may consist of an array of segments that are kinematically the same as a single fault, therefore recognizing a distinction between faults and fault segments. The role of linkage between faults or fault segments in the formation of larger faults became the focus of later studies (e.g. Peacock & Sanderson 1991; Cartwright *et al.* 1995).

Conceptual models of the growth of a single fault from an initial array of smaller faults or fault segments are illustrated in Figure 1 (similar figures can be found in **Nicol *et al.* 2016**; **Morley 2016**; **Finch & Gawthorpe 2017**; **Jackson *et al.* 2017**). Three different models are distinguished based on two criteria. These criteria are: first, whether the initial faults formed as elements within a coherent structure or whether they formed in mechanical and kinematic isolation from one another (coherent v. non-coherent in Fig. 1); and second, whether the faults established their lengths at low displacements or whether there was a protracted period of fault propagation during displacement accumulation (constant-length v. propagating in Fig. 1).

Figure 1a illustrates the non-coherent case with three initially unconnected faults that are broadly aligned along-strike, but are kinematically unrelated to one another. As their displacement increases, the faults become longer until they interact with one another preventing, or at least retarding, further propagation, as reflected by increased displacement gradients at the boundaries between the faults (i.e. at the relay zones). As the displacement increases further, the faults become connected or linked to form a single large fault with associated splays. The displacement distribution on the resultant through-going fault is irregular, with local displacement lows at the sites of former segment boundaries. However, the characteristic feature of this model is the irregularity of the profile of the total, or aggregate, fault displacement, with local displacement highs and lows recording the earlier presence of separate, previously isolated, faults.

Figure 1b, c illustrate the cases in which geometric coherence is maintained throughout the growth of a fault. Geometric coherence is illustrated by the simple triangular profile of aggregate displacement, which demonstrates that the individual fault segments are part of a single larger structure (Walsh & Watterson 1991) even though they are not geometrically connected at the scale of observation (i.e. not hard-linked). Instead, soft linkage allows coherence of the large-scale fault displacement through distributed strain accommodated within the adjacent wall rock. Although the displacement distribution on the through-going fault

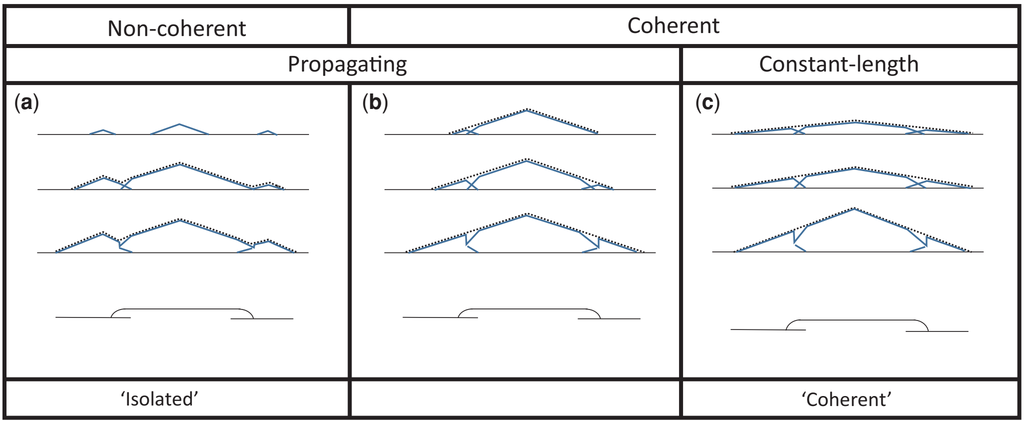

Fig. 1. Displacement-length profiles illustrating three potential growth histories leading to the same fault map pattern. The solid lines are the displacement profiles for individual faults and the dashed lines are profiles of aggregate displacement. The three cases are distinguished on the basis of whether the faults are coherent and whether the faults propagate continuously as displacement increases. The non-coherent propagating case is commonly referred to as the 'isolated' model and the constant-length coherent case is commonly referred to as the 'coherent' model. The propagating coherent case is also possible, but is less commonly invoked. The evolution of the fault traces for parts (a) and (c) are illustrated in Figure 2. The profiles shown are for normal faults in map view, but similar considerations are equally applicable to faults in cross-section.

is again irregular, with lows at the locations of the initial segment boundaries, in this case the profile of aggregate displacement has a simple triangular shape, in which lows on the through-going fault are fully compensated by displacements on splays and bed rotations. In Figure 1b the geometrically coherent fault array propagates as displacement accumulates and new segments formed at the tip of the propagating fault are part of the larger structure from the outset. In Figure 1c the fault trace lengths are established in the first growth increment and subsequent fault propagation occurs only during linkage between segments.

A variety of terms have been applied to these models. The model illustrated in Figure 1a is widely referred to as the 'isolated' fault model, reflecting the fact that individual faults within an array of faults can initiate as kinematically isolated structures at random locations, eventually coalescing to form a large fault by incidental interaction and linkage. This contrasts with 'coherent' fault models, where fault segments initiate as elements within a larger structure. The existence of a larger structure is most clearly illustrated for arrays of fault segments seen in map or cross-section that connect to a single fault in the third dimension (Walsh *et al.* 2003).

Although it is possible to distinguish between faults and fault segments that developed according to the isolated and coherent models based on finite displacement distributions, distinguishing between the constant-length and propagating variants of the coherent model requires the back-stripping of displacements to determine whether there was a protracted period of fault propagation. In principle, arrays of fault segments could progressively propagate laterally (the coherent propagating model of Fig. 1b), but this type of behaviour is much less commonly advocated than the isolated (Fig. 1a) and the constant-length coherent (Fig. 1c) models, which are therefore generally considered to be end-member fault growth cases.

Growth of fault systems

The models and concepts described for the growth of individual faults are broadly equivalent to those used to describe the growth of fault systems. Although discussions on the development of individual faults have largely centred on the difference between the isolated and coherent models (e.g. Jackson & Rotevatn 2013), recent discussions on the growth of fault systems have focused more specifically on the distinction between the isolated and the constant-length coherent model. These two models are illustrated on the schematic maps in Figure 2 and fault displacement distributions from each are shown in Figure 1a and c, respectively. In the isolated model, faults are initially randomly located and kinematically independent of one another. Faults grow by progressive propagation and by the interaction and coalescence of fortuitously aligned smaller faults; one such fault and its displacement evolution is shown in Figure 1a. According to this model, the established positive correlation between fault displacement and length defines the trend that individual faults follow as they accrue displacement and lengthen (Fig. 2f). This model and variants of it have been referred to as the isolated fault model (e.g. **Ghalayini *et al.* 2016**; **Morley 2016**), the standard fault model (Walsh *et al.* 2002) and the increasing length fault model (**Nicol *et al.* 2016**). The term 'isolated fault model' is most widely used in the current literature and describes the defining feature that faults initiate as spatially and kinematically isolated structures.

According to the constant-length, coherent model for fault system evolution, fault trace lengths and interactions between faults are established at low strains and subsequent fault propagation is limited to the linkage between adjacent faults. The associated displacement distribution through time is illustrated in Figure 1c. The D–L growth curve followed by an individual fault in this case is in two portions (Fig. 2f) separated by a bend, where a growing fault changes from rapid propagation at low strain to the accumulation of displacement without significant propagation. This model has been referred to as the alternative model (Walsh *et al.* 2002), the coherent model (**Morley 2016**) and the constant-length model (Curry *et al.* 2016; **Nicol *et al.* 2016**; **Jackson *et al.* 2017**), with the last two becoming the most commonly used in the recent literature. Here we refer to it as the constant-length coherent fault model.

The description of these models is simplified here and, for example, we do not represent the stepwise increase in fault length associated with fault linkage in the isolated fault model in Figure 2e. Similarly, we illustrate these models on two-dimensional map view sections partly for simplicity, but also because the best available constraints on fault growth currently come from studies of syn-faulting sedimentation, which provide information on the surface trace lengths of faults; both models can be considered in three dimensions with faults that propagate out of the plane of observation. For the purpose of clarity, the two models for the growth of fault systems are starkly contrasted here, but conceptually they represent end-members in a range of possible behaviours. For example, as extension increases within fault systems originally subscribing to the constant-length model, there will be a progressive increase in D/L ratios on individual faults, eventually leading to the linkage of adjacent faults. Although this is reminiscent of the isolated fault model, it differs in the crucial respect that the fault

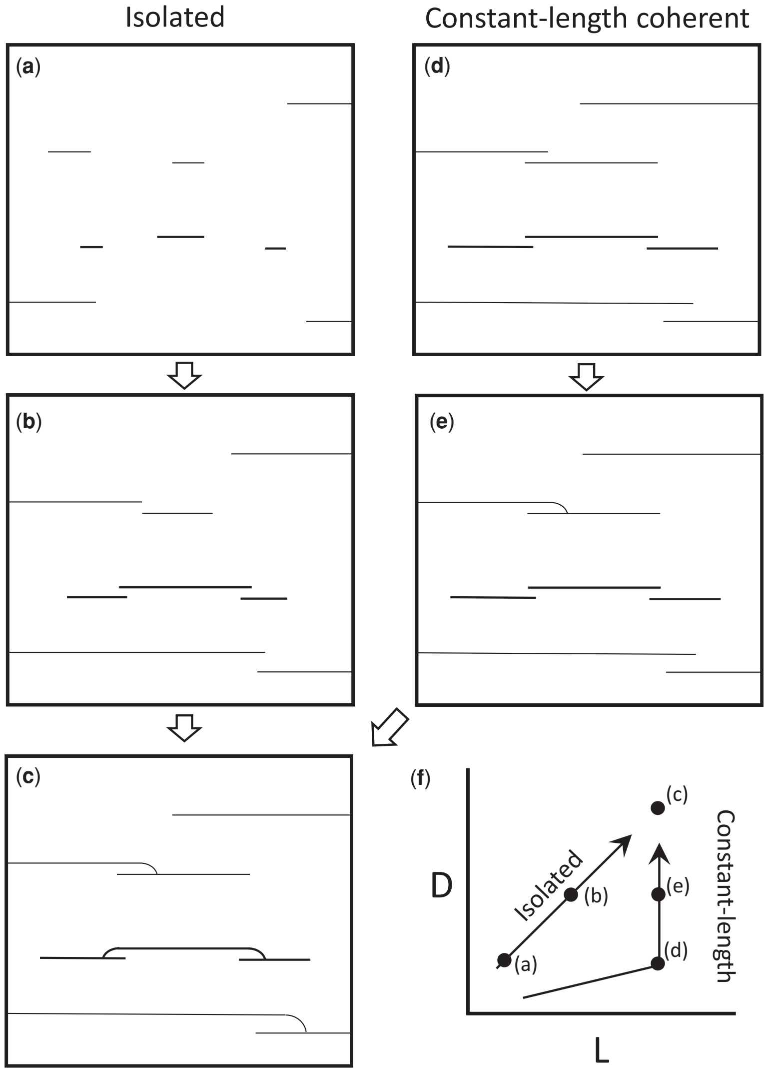

Fig. 2. Schematic maps illustrating how the isolated (**a**, **b**) and constant-length coherent (**d**, **e**) models of fault growth can give rise to the same fault map pattern (**c**). The displacement profiles through time for the faults highlighted in bold are shown in Figure 1.

map is effectively established very early apart from the linkage of adjacent faults at higher strains. Many of the papers in this volume do not specifically address these models of fault growth, but most do make directly relevant geometrical observations on displacement distributions on faults. Several papers directly address these growth models, either from a study of faults that intersect growth strata (**Morley 2016**; **Worthington & Walsh 2016**; **Jackson *et al.* 2017**), from finite displacement profile data (**Ghalayini *et al.* 2016**; **Homberg *et al.* 2017**) or from modelling (**Whipp *et al.* 2016**; **Finch & Gawthorpe 2017**), and invoke one or other of the isolated or constant-length coherent models.

Temporal resolution

The two fault growth models can be viewed as end-members of a spectrum of behaviours. For example, the simple map view cartoon in Figure 2d shows that all faults achieve their length in the first increment of fault growth. There is clearly a finite period in which these faults propagate through the rock volume to establish their lengths, but the duration of this period is difficult to establish. Sediment thickness data may show that faults are established in the first resolvable time increment, but in some cases this increment may be millions of years. Similarly, for the isolated fault model there is a time when all faults have propagated to interact with adjacent faults and the subsequent formation of new fault trace lengths is predominantly by fault linkage. The key distinction between the models is therefore how quickly, or at what strain, the transition from behaviour dominated by fault propagation to behaviour dominated by fault interaction occurs. Taylor *et al.* (2004), for example, suggested that this transition occurred *c.* 700 ka after fault initiation. Analysis of an Australian NW shelf dataset described by Walsh *et al.* (2002) shows that this transition occurred over <500 ka and at very low strains (<3%). In the clay models of **Whipp *et al.* (2016)**, the early stages of fault growth are dominated by isolated faults that propagate and grow towards one another; the development of the model fault systems is considered to adhere to the isolated fault model. However, in these models, *c.* 95% of the fault length is established in a strain interval from 10 to 25% extension, with subsequent growth accommodated by an increase in displacement without further propagation.

Fault-related folding

For most fault systems, geological conditions and/or the available data preclude direct study of fault growth histories. In these situations, it may be possible to distinguish between the isolated and coherent models based on whether mapped displacement profiles resemble that in Figure 1a (or Fig. 1b or c). The key difference between the isolated and coherent models is the shape of the total or aggregate throw profile. Accurate definition of this profile can be difficult, primarily due to the ductile component of displacement that accompanies faulting. The interchange between faulting and folding, or discontinuous and continuous deformation, within geological structures is well established and several contributions to this volume address this topic (e.g. **Childs *et al.* 2016**; **Delogkos *et al.* 2016**; **Fazlikhani *et al.* 2016**; **Ferrill *et al.* 2016**; **Lăpădat *et al.* 2016**; **Homberg *et al.* 2017**). Within normal fault systems, continuous deformation occurs primarily as monoclines related to fault tip propagation and as bed rotations within relay zones separating adjacent fault segments (**Childs *et al.* 2016**; **Lăpădat *et al.* 2016**; **Khalil & McClay 2016**). Using detailed outcrop and seismic mapping, these papers show that arrays of fault segments are often accompanied by associated folding, particularly adjacent to relay zones, highlighting the interchangeability of folding and faulting through time within a single kinematic structure. Bed rotations within relay zones can occur at relay ramps seen in map view or at sites of vertical segmentation (**Roche *et al.* 2016**; **Homberg *et al.* 2017**). Irrespective of the origin of fault-related continuous deformation, it represents an integral part of the total displacement across a fault and failure to include this component can result in false lows on profiles of aggregate displacement and hence to the erroneous attribution to the isolated model.

Boundary conditions and pre-existing structures

Idealized models for the growth of fault systems are described in the context of simplified considerations of a volume of rock subjected to uniform extension (e.g. Fig. 2, **Finch & Gawthorpe 2017**; **Whipp *et al.* 2016**). In reality, such simple boundary conditions rarely apply and, for example, the magnitude of extension may vary along strike, or the extended crust may be strongly heterogeneous (Jackson & Rotevatn 2013; **Ferrer *et al.* 2016**; **Ferrill *et al.* 2016**). The departure from idealized models of fault system evolution is addressed in several contributions to this volume. **Ford *et al.* (2016)** provide detailed evidence for two phases of propagation of faults bounding the Gulf of Corinth. This propagation is attributed to a change in the tectonic control on local extension rate. Many earlier studies (e.g. Morley 2002; Noll & Hall 2006) have demonstrated lateral changes in the focus for extension, which again is generally attributed to changes in boundary conditions. Changes in displacement rates along the lengths of faults may also be driven by internal changes in the geometry of the active fault system as it evolves – for example, as a fault system becomes progressively polarized into one dominant dip direction (Nixon *et al.* 2016; **Finch & Gawthorpe 2017**). **Morley (2016)** shows how displacement profiles for a large boundary fault record progressive migration in activity along strike, pointing to the fact that the resultant displacement distribution is not consistent with either of the simple current models of fault growth. Sandbox modelling of listric fault geometries provides a clear rationale for the migration of the locations of active faulting (**Ferrer *et al.* 2016**).

The constant-length coherent fault model was first formally described for normal faults that reactivate earlier underlying fault systems, where the extension directions of the early and late rifting phases were subparallel (Walsh *et al.* 2002). In this case, the rapid development of very long fault traces with low displacements in the cover sequence occurred because these fault lengths were already established in the pre-rift section during the previous extensional phase and, during subsequent reactivation, propagated upwards to intersect the free surface. Walsh *et al.* (2002) also pointed out, however, that the rapid development of fault lengths could even apply to faults that are not reactivated because there was, and still is, little direct published kinematic evidence for slow progressive growth in fault length. In an earlier study, Morley (1999) described basin-bounding faults in the East African Rift that showed rapid and early propagation, without invoking a role for pre-existing structures. Nevertheless, similar, more recent, studies demonstrating a constant-length coherent model have recognized a significant control of underlying structure (e.g. Paton 2006; Jackson & Rotevatn 2013). There is therefore little doubt that an optimally oriented pre-existing structure favours rapid fault propagation, but this could often be the case given the presence of older structure in many newly formed basins. Conversely, the extent to which the isolated model could apply in 'virgin' crust is difficult to ascertain because many basins are developed in crust that has been deformed during earlier phases of deformation (whether in extension or compression).

The significance of pre-existing structure on fault system evolution, both in extension and compression, is the subject of several contributions to this volume. **Worthington & Walsh (2016)** present an example of a reactivated basement fault in which upwards propagation provides a geometrically coherent array of fault segments characterized by very rapid and, effectively constant, fault trace lengths in the cover. In this case, coherence is achieved by soft linkage in map view and hard linkage into a single fault at depth. **Reilly *et al.* (2016)** provide an example of the reverse reactivation of earlier normal faults and show that only the largest faults in the extensional system become reactivated and that this reactivation is generally along the full fault length. **Morley (2016)** describes how multiple superposed extension events result in both over- and under-displaced faults with displacement variations that are not readily assigned to any one model of fault growth. **Fossen *et al.* (2016)** document how the presence of Caledonian structure and Devonian extensional faults mapped onshore Norway can be extrapolated offshore, where they control the geometries of later Triassic and Jurassic rifting. They discuss how pre-existing structure determines the development of different structural domains within an evolving fault system. By contrast, analogue (**Whipp *et al.* 2016**) and numerical (**Finch & Gawthorpe 2017**) modelling show that different structural domains characterized by opposed fault polarity and separated by distinct boundaries can also emerge from extension of a homogeneous medium.

The selection of papers in this volume show that the boundary conditions and pre-existing crustal structure can have a significant impact on the geometry and growth histories of faults, an issue which explains why it can sometimes be challenging to determine the generic characteristics of fault growth from studies of particular areas with different geological and tectonic settings.

Fault zone structure and evolution

Patterns of minor faults and damage zones associated with normal faults, including correlations between the widths of damage zones and fault displacement, have previously been used to underpin models of fault zone growth (e.g. Shipton & Cowie 2003; Fossen *et al.* 2007). **Skar *et al.* (2016)** find no correlation between damage zone width and displacement for faults with throws in the range 0.6–30 m, but find that the variation in the measured damage zone width on a single fault is greater than between faults of different displacement. **Nicol *et al.* (2016)** make the outcrop observation that fault tips are often characterized by the splaying of faults, but the splays that might be expected along the lengths of faults at former tip locations are absent. This observation suggests that the studied faults established their lengths rapidly and form geometrically coherent arrays. **Roche *et al.* (2016)** recognize a similar increase in fault zone complexity at fault tips and develop a model in which the locally increased thickness of fault zones can be attributed to the arrest of bed-normal propagation at less competent units within a layered sequence. Numerical modelling of the growth of normal faults by **Schöpfer *et al.* (2016)** focuses on the localization of strain within a fracture array established at very low strains. The width of the initial zone of fracture is largely independent of the mechanical properties of the model, but the localization of strain onto a single fault within the zone as displacement accrues is strongly dependent on the mechanical properties of the faulted sequence.

Fault growth studies generally concentrate on how fault surfaces achieve their lengths and displacements. A closely related topic is the internal structure of fault zones and there is considerable overlap between these two topics. This is particularly clear where, for example, relay zones between segments of an array of normal faults are breached and the relay zone is preserved as a splay or a lens within a fault zone (e.g. **Whipp *et al.* 2016**). Studies of the internal structure of fault zones can therefore shed light on fault growth. **Yielding (2016)** details the relationship between the orientations of branch lines between faults, and between slip-surfaces within fault zones, and relates them to style of faulting and extension direction. **Childs *et al.* (2016)** present a model relating the geometry of segment boundaries and, in particular, the associated folding (often reflected as normal drag) to the fault zone internal structure that results as displacement increases. **Gabrielsen *et al.* (2016)** examine the internal structure of faults at higher strains, where former segment boundaries may be preserved as lenses within fault zones.

Geometry and growth of normal faults

This volume of papers was compiled following a conference of the same title held at the Geological Society of London in 2014 in honour of Juan Watterson. The topic of the conference was chosen to reflect Juan's interests and his significant contribution to our understanding of the growth of faults. Juan was a firm believer in the analysis of strain as a means of understanding the evolution of geological structures and he pioneered the development of various quantitative methods related to displacement and strain that explored the nature of fault growth. His view was that stresses and forces can only be speculated for ancient events and, because we deal with large observable strains, much more progress can be made if structural geologists have a cultural disposition towards geometry, displacement and strain. In that sense, he subscribed to the view of Burland (1965) (quoted in Roscoe 1970), that 'stress is a philosophical concept, deformation is a physical reality'. The availability of improved constraints from earthquake studies and advances in numerical modelling techniques are, however, helping us to address stress-related issues and their implications for fault growth on geological timescales. Although Juan would have been supportive, and perhaps at the vanguard, of the adoption of new approaches, he still would have been a strong advocate of the acquisition and analysis of the best three-dimensional geological datasets, ideally from fieldwork, to resolve outstanding scientific questions. In that sense, Juan would have been delighted to read this volume because it reveals interesting and new insights on fault growth by the application of established and new methods. It would not have been in his nature to solicit credit for his work, but the involvement of many of the world's experts in this volume reflects the importance of his contributions and the respect with which he is held.

References

Burland, J.B. 1965. *Deformation of soft clay*. PhD thesis, University of Cambridge.

Cartwright, J.A., Trudgill, B.D. & Mansfield, C.S. 1995. Fault growth by segment linkage: an explanation for scatter in maximum displacement and trace length data from the Canyonlands Grabens of SE Utah. *Journal of Structural Geology*, **17**, 1319–1326.

Childs, C., Nicol, A., Walsh, J.J. & Watterson, J. 2003. The growth and propagation of synsedimentary faults. *Journal of Structural Geology*, **25**, 633–648.

Childs, C., Manzocchi, T., Nicol, A., Walsh, J.J., Soden, A.M., Conneally, J.C. & Delogkos, E. 2016. The relationship between normal drag, relay ramp aspect ratio and fault zone structure. *In*: Childs, C., Holdsworth, R.E., Jackson, C.A.-L., Manzocchi, T., Walsh, J.J. & Yielding, G. (eds) *The Geometry and Growth of Normal Faults*. Geological Society, London, Special Publications, **439**. First published online August 17, 2016, https://doi.org/10.1144/SP439.16

Cowie, P.A. & Scholz, C.H. 1992. Displacement-length scaling relationship for faults: data synthesis and discussion. *Journal of Structural Geology*, **14**, 1149–1156.

Curry, M.A., Barnes, J.B. & Colgan, J.P. 2016. Testing fault growth models with low-temperature thermochronology in the northwest Basin and Range, USA. *Tectonics*, **35**, 2467–2492.

Dawers, N.H., Anders, M.H. & Scholz, C.H. 1993. Fault length and displacement: scaling laws. *Geology*, **21**, 1107–1110.

Delogkos, E., Manzocchi, T. *et al.* 2016. Throw partitioning across normal fault zones in the Ptolemais Basin, Greece. *In*: Childs, C., Holdsworth, R.E., Jackson, C.A.-L., Manzocchi, T., Walsh, J.J. & Yielding, G. (eds) *The Geometry and Growth of Normal Faults*. Geological Society, London, Special Publications, **439**. First published online November 21, 2016, https://doi.org/10.1144/SP439.19

Elliott, D. 1976. The energy balance and deformation mechanisms of thrust sheets. *Philosophical Transactions of the Royal Society of London A: Mathematical, Physical and Engineering Sciences*, **283**, 289–312.

Fazlikhani, H., Back, S., Kukla, P.A. & Fossen, H. 2016. Interaction between gravity-driven listric normal fault linkage and their hanging-wall rollover development: a case study from the western Niger Delta, Nigeria. *In*: Childs, C., Holdsworth, R.E., Jackson, C.A.-L., Manzocchi, T., Walsh, J.J. & Yielding, G. (eds) *The Geometry and Growth of Normal Faults*. Geological Society, London, Special Publications, **439**. First published online December 13, 2016, https://doi.org/10.1144/SP439.20

Ferrer, O., McClay, K. & Sellier, N.C. 2016. Influence of fault geometries and mechanical anisotropies on the growth and inversion of hanging-wall synclinal basins: insights from sandbox models and natural examples. *In*: Childs, C., Holdsworth, R.E., Jackson, C.A.-L., Manzocchi, T., Walsh, J.J. & Yielding, G. (eds) *The Geometry and Growth of Normal Faults*. Geological Society, London, Special Publications, **439**. First published online March 15, 2016, https://doi.org/10.1144/SP439.8

Ferrill, D.A., Morris, A.P., McGinnis, R.N. & Smart, K.J. 2016. Myths about normal faulting. *In*: Childs, C., Holdsworth, R.E., Jackson, C.A.-L., Manzocchi, T., Walsh, J.J. & Yielding, G. (eds) *The Geometry and Growth of Normal Faults*. Geological Society, London, Special Publications, **439**. First published online March 30, 2016, https://doi.org/10.1144/SP439.12

Finch, E. & Gawthorpe, R. 2017. Growth and interaction of normal faults and fault network evolution in rifts: insights from three-dimensional discrete element modelling. *In*: Childs, C., Holdsworth, R. E., Jackson, C. A.-L., Manzocchi, T., Walsh, J. J. & Yielding, G. (eds) *The Geometry and Growth of Normal Faults*. Geological Society, London, Special Publications, **439**. First published online August 30, 2017, https://doi.org/10.1144/SP439.23

Ford, M., Hemelsdaël, R., Mancini, M. & Palyvos, N. 2016. Rift migration and lateral propagation: evolution of normal faults and sediment-routing systems of the western Corinth rift (Greece). *In*: Childs, C., Holdsworth, R.E., Jackson, C.A.-L., Manzocchi, T., Walsh, J.J. & Yielding, G. (eds) *The Geometry and Growth of Normal Faults*. Geological Society, London, Special Publications, **439**. First published online August 15, 2016, https://doi.org/10.1144/SP439.15

Fossen, H., Schultz, R.A., Shipton, Z.K. & Mair, K. 2007. Deformation bands in sandstone: a review. *Journal of the Geological Society*, **164**, 755–769.

Fossen, H., Fazli Khani, H., Faleide, J.I., Ksienzyk, A.K. & Dunlap, W.J. 2016. Post-Caledonian extension in the West Norway–northern North Sea region: the role of structural inheritance. *In*: Childs, C., Holdsworth, R.E., Jackson, C.A.-L., Manzocchi, T., Walsh, J.J. & Yielding, G. (eds) *The Geometry and Growth of Normal Faults*. Geological Society, London, Special Publications, **439**. First published online February 5, 2016, https://doi.org/10.1144/SP439.6

Gabrielsen, R.H., Braathen, A., Kjemperud, M. & Valdresbråten, M.L.R. 2016. The geometry and dimensions of fault-core lenses. *In*: Childs, C., Holdsworth, R.E., Jackson, C.A.-L., Manzocchi, T., Walsh, J.J. & Yielding, G. (eds) *The Geometry and Growth of Normal Faults*. Geological Society, London, Special Publications, **439**. First published online February 5, 2016, https://doi.org/10.1144/SP439.4

Ghalayini, R., Homberg, C., Daniel, J.M. & Nader, F.H. 2016. Growth of layer-bound normal faults under a regional anisotropic stress field. *In*: Childs, C., Holdsworth, R.E., Jackson, C.A.-L., Manzocchi, T., Walsh, J.J. & Yielding, G. (eds) *The Geometry and Growth of Normal Faults*. Geological Society, London, Special Publications, **439**. First published online April 6, 2016, https://doi.org/10.1144/SP439.13

Gillespie, P.A., Walsh, J.J. & Watterson, J. 1992. Limitations of dimension and displacement data from single faults and the consequences for data analysis and interpretation. *Journal of Structural Geology*, **14**, 1157–1172.

Homberg, C., Schnyder, J., Roche, V., Leonardi, V. & Benzaggagh, M. 2017. The brittle and ductile components of displacement along fault zones. *In*: Childs, C., Holdsworth, R.E., Jackson, C.A.-L., Manzocchi, T., Walsh, J.J. & Yielding, G. (eds) *The Geometry and Growth of Normal Faults*. Geological Society, London, Special Publications, **439**. First published online March 1, 2017, https://doi.org/10.1144/SP439.21

Jackson, C.A.L. & Rotevatn, A. 2013. 3D seismic analysis of the structure and evolution of a salt-influenced normal fault zone: a test of competing fault growth models. *Journal of Structural Geology*, **54**, 215–234.

Jackson, C.A.-L., Bell, R.E., Rotevatn, A. & Tvedt, A.B.M. 2017. Techniques to determine the kinematics of synsedimentary normal faults and implications for fault growth models. *In*: Childs, C., Holdsworth, R.E., Jackson, C.A.-L., Manzocchi, T., Walsh, J.J. & Yielding, G. (eds) *The Geometry and Growth of Normal Faults*. Geological Society, London, Special Publications, **439**. First published online February 7, 2017, https://doi.org/10.1144/SP439.22

Kakimi, T. 1980. Magnitude-frequency relation for displacement of minor faults and its significance in crustal deformation. *Bulletin of the Geological Survey of Japan*, **31**, 467–487.

Khalil, S.M. & McClay, K.R. 2016. 3D geometry and kinematic evolution of extensional fault-related folds, NW Red Sea, Egypt. *In*: Childs, C., Holdsworth, R.E., Jackson, C.A.-L., Manzocchi, T., Walsh, J.J. & Yielding, G. (eds) *The Geometry and Growth of Normal Faults*. Geological Society, London, Special Publications, **439**. First published online March 30, 2016, https://doi.org/10.1144/SP439.11

Kim, Y.-S. & Sanderson, D.J. 2005. The relationship between displacement and length of faults: a review. *Earth-Science Reviews*, **68**, 317–334.

Lăpădat, A., Imber, J., Yielding, G., Iacopini, D., McCaffrey, K.J.W., Long, J.J. & Jones, R.R. 2016. Occurrence and development of folding related to normal faulting within a mechanically heterogeneous sedimentary sequence: a case study from Inner Moray Firth, UK. *In*: Childs, C., Holdsworth, R.E., Jackson, C.A.-L., Manzocchi, T., Walsh, J.J. & Yielding, G. (eds) *The Geometry and Growth of Normal Faults*. Geological Society, London, Special Publications, **439**. First published online September 26, 2016, https://doi.org/10.1144/SP439.18

Marrett, R. & Allmendinger, R.W. 1992. Amount of extension on 'small' faults: an example from the Viking graben. *Geology*, **20**, 47–50.

Morley, C.K. 1999. Patterns of displacement along large normal faults: implications for basin evolution and fault propagation, based on examples from East Africa. *AAPG Bulletin*, **83**, 613–634.

Morley, C.K. 2002. Evolution of large normal faults: evidence from seismic reflection data. *AAPG Bulletin*, **86**, 961–978.

Morley, C.K. 2016. The impact of multiple extension events, stress rotation and inherited fabrics on normal fault geometries and evolution in the Cenozoic rift basins of Thailand. *In*: Childs, C., Holdsworth, R.E., Jackson, C.A.-L., Manzocchi, T., Walsh, J.J. & Yielding, G. (eds) *The Geometry and Growth of Normal Faults*. Geological Society, London, Special Publications, **439**. First published online April 13, 2016, https://doi.org/10.1144/SP439.3

Nicol, A., Childs, C., Walsh, J.J., Manzocchi, T. & Schöpfer, M.P.J. 2016. Interactions and growth of faults in an outcrop-scale system. *In*: Childs, C., Holdsworth, R.E., Jackson, C.A.-L., Manzocchi, T., Walsh, J.J. & Yielding, G. (eds) *The Geometry and Growth of Normal Faults*. Geological Society, London, Special Publications, **439**. First published online March 10, 2016, https://doi.org/10.1144/SP439.9

Nixon, C.W., McNeill, L.C. *et al.* 2016. Rapid spatio-temporal variations in rift structure during development of the Corinth Rift, central Greece. *Tectonics*, **35**, 1225–1248.

Noll, C.A. & Hall, M. 2006. Normal fault growth and its function on the control of sedimentation during basin formation: a case study from field exposures of the Upper Cambrian Owen Conglomerate, West Coast Range, western Tasmania, Australia. *AAPG Bulletin*, **90**, 1609–1630.

Paton, D.A. 2006. Influence of crustal heterogeneity on normal fault dimensions and evolution: southern South Africa extensional system. *Journal of Structural Geology*, **28**, 868–886.

Peacock, D.C.P. & Sanderson, D.J. 1991. Displacements, segment linkage and relay ramps in normal fault zones. *Journal of Structural Geology*, **13**, 721–733.

Reilly, C., Nicol, A. & Walsh, J. 2016. Importance of pre-existing fault size for the evolution of an inverted fault system. *In*: Childs, C., Holdsworth, R.E., Jackson, C.A.-L., Manzocchi, T., Walsh, J.J. & Yielding, G. (eds) *The Geometry and Growth of Normal Faults*. Geological Society, London, Special Publications, **439**. First published online February 5, 2016, https://doi.org/10.1144/SP439.2

Roche, V., Homberg, C., van der Baan, M. & Rocher, M. 2016. Widening of normal fault zones due to the inhibition of vertical propagation. *In*: Childs, C., Holdsworth, R.E., Jackson, C.A.-L., Manzocchi, T., Walsh, J.J. & Yielding, G. (eds) *The Geometry and Growth of Normal Faults*. Geological Society, London, Special Publications, **439**. First published online February 5, 2016, https://doi.org/10.1144/SP439.5

Roscoe, K.H. 1970. The influence of strains on soil mechanics. *Geotechnique*, **20**, 129–170.

Schöpfer, M.P.J., Childs, C., Manzocchi, T. & Walsh, J.J. 2016. Three-dimensional distinct element method modelling of the growth of normal faults in layered sequences. *In*: Childs, C., Holdsworth, R.E., Jackson, C.A.-L., Manzocchi, T., Walsh, J.J. & Yielding, G. (eds) *The Geometry and Growth of Normal Faults*. Geological Society, London, Special Publications, **439**. First published online September 15, 2016, https://doi.org/10.1144/SP439.17

Schultz, R.A., Soliva, R., Fossen, H., Okubo, C.H. & Reeves, D.M. 2008. Dependence of displacement–length scaling relations for fractures and deformation bands on the volumetric changes across them. *Journal of Structural Geology*, **30**, 1405–1411.

Shipton, Z.K. & Cowie, P.A. 2003. A conceptual model for the origin of fault damage zone structures in high-porosity sandstone. *Journal of Structural Geology*, **25**, 333–344.

Skar, T., Berg, S.S., Gabrielsen, R.H. & Braathen, A. 2016. Fracture networks of normal faults in fine-grained sedimentary rocks: examples from Kilve Beach, SW England. *In*: Childs, C., Holdsworth, R.E., Jackson, C.A.-L., Manzocchi, T., Walsh, J.J. & Yielding, G. (eds) *The Geometry and Growth of Normal Faults*. Geological Society, London, Special Publications, **439**. First published online September 26, 2016, https://doi.org/10.1144/SP439.10

Taylor, S.K., Bull, J.M., Lamarche, G. & Barnes, P.M. 2004. Normal fault growth and linkage in the Whakatane Graben, New Zealand, during the last 1.3 Myr. *Journal of Geophysical Research: Solid Earth*, **109**, B02408.

Walsh, J.J. & Watterson, J. 1988. Analysis of the relationship between displacements and dimensions of faults. *Journal of Structural Geology*, **10**, 239–247.

Walsh, J.J. & Watterson, J. 1989. Displacement gradients on fault surfaces. *Journal of Structural Geology*, **11**, 307–316.

Walsh, J.J. & Watterson, J. 1991. Geometric and kinematic coherence and scale effects in normal fault systems. *In*: Roberts, A.M., Yielding, G. & Freeman, B. (eds) *The Geometry of Normal Faults*. Geological Society, London, Special Publications, **56**, 193–203, https://doi.org/10.1144/GSL.SP.1991.056.01.13

Walsh, J.J., Watterson, J. & Yielding, G. 1991. The importance of small-scale faulting in regional extension. *Nature*, **351**, 391–393.

Walsh, J.J., Nicol, A. & Childs, C. 2002. An alternative model for the growth of faults. *Journal of Structural Geology*, **24**, 1669–1675.

Walsh, J.J., Bailey, W.R., Childs, C., Nicol, A. & Bonson, C.G. 2003. Formation of segmented normal faults: a 3-D perspective. *Journal of Structural Geology*, **25**, 1251–1262.

Watterson, J. 1986. Fault dimensions, displacements and growth. *Pure and Applied Geophysics*, **124**, 365–373.

Whipp, P.S., Jackson, C.A.-L., Schlische, R.W., Withjack, M.O. & Gawthorpe, R.L. 2016. Spatial distribution and evolution of fault-segment boundary types in rift systems: observations from experimental clay models. *In*: Childs, C., Holdsworth, R.E., Jackson, C.A.-L., Manzocchi, T., Walsh, J.J. & Yielding, G. (eds) *The Geometry and Growth of Normal Faults*. Geological Society, London, Special Publications, **439**. First published online March 31, 2016, https://doi.org/10.1144/SP439.7

Wojtal, S.F. 1994. Fault scaling laws and the temporal evolution of fault systems. *Journal of Structural Geology*, **16**, 603–612.

Worthington, R.P. & Walsh, J.J. 2016. Timing, growth and structure of a reactivated basin-bounding fault. *In*: Childs, C., Holdsworth, R.E., Jackson, C.A.-L., Manzocchi, T., Walsh, J.J. & Yielding, G. (eds) *The Geometry and Growth of Normal Faults*. Geological Society, London, Special Publications, **439**. First published online July 1, 2016, https://doi.org/10.1144/SP439.14

Yielding, G. 2016. The geometry of branch lines. *In*: Childs, C., Holdsworth, R.E., Jackson, C.A.-L., Manzocchi, T., Walsh, J.J. & Yielding, G. (eds) *The Geometry and Growth of Normal Faults*. Geological Society, London, Special Publications, **439**. First published online February 22, 2016, https://doi.org/10.1144/SP439.1